

*In situ* ferromagnetic resonance in coupled ultrathin trilayers with perpendicularly oriented easy axes

This article has been downloaded from IOPscience. Please scroll down to see the full text article.

2003 J. Phys.: Condens. Matter 15 7175

(<http://iopscience.iop.org/0953-8984/15/43/003>)

View [the table of contents for this issue](#), or go to the [journal homepage](#) for more

Download details:

IP Address: 171.66.16.125

The article was downloaded on 19/05/2010 at 17:38

Please note that [terms and conditions apply](#).

# *In situ* ferromagnetic resonance in coupled ultrathin trilayers with perpendicularly oriented easy axes

K Lenz<sup>1</sup>, E Kosubek, T Toliński<sup>2</sup>, J Lindner and K Baberschke

Institut für Experimentalphysik, Freie Universität Berlin, Arnimallee 14, D-14195 Berlin, Germany

E-mail: babgroup@physik.fu-berlin.de

Received 9 July 2003

Published 17 October 2003

Online at [stacks.iop.org/JPhysCM/15/7175](http://stacks.iop.org/JPhysCM/15/7175)

## Abstract

Ultrathin ferromagnetic trilayers with perpendicularly oriented easy axes—one film in-plane the other out-of-plane—attracted recent interest in the study of interlayer exchange coupling, domain formation, and canted magnetization orientation. To investigate and understand the thermodynamic ground state of such a prototype trilayer we employed *in situ* ferromagnetic resonance (FMR) for a Ni/Cu/Co/Cu(001) trilayer. The FMR polar angular dependence has been measured and analysed in the framework of the Landau–Lifshitz equation. In addition the thickness of the Cu spacer layer has been changed to manipulate the strength of the interlayer exchange coupling and select between ferromagnetic and antiferromagnetic coupling. The FMR experiment yields—unlike other techniques—the coupling strength and anisotropy energy in absolute energy units. This gives also a full insight into all the parameters governing the ground state free energy, the equilibrium angles of the canted magnetization, as well as the optical and acoustical mode formed by the two uniform spin-wave excitations.

## 1. Introduction

The magnetic properties and the interlayer exchange coupling  $J_{\text{inter}}$  of trilayers for various combinations of ferromagnetic (FM) elements, like Co, Ni, etc, separated by a non-magnetic metallic spacer layer (e.g. Cu) have been the focus of thorough investigations in recent years [1–11]. Particular interest has been paid to the case where the FM layers consist of films with thicknesses  $d$  far below the so-called ultrathin limit for which  $d$  is smaller than the exchange length. In this regime the spins within the FM layers are rigidly coupled, thus behaving as a giant magnetic moment. The importance of such an ultrathin film lies in the fact that the orientation

<sup>1</sup> Author to whom any correspondence should be addressed.

<sup>2</sup> Permanent address: Institute of Molecular Physics, PAS, Smoluchowskiego 17, 60-179 Poznań, Poland.

of its easy axis can easily be manipulated by diverse parameters, e.g. the thickness, the interface topology, surfactants, or by using a cap layer. However, studies have mainly considered the case where *both* magnetizations have orientations parallel to either the in-plane or out-of-plane direction [2–6]. Recent principal interest focuses on films with perpendicular alignment of the two ferromagnets, i.e. one film in-plane, the second out-of-plane. Such systems have been studied in the as-grown state [9, 10] and in remanence [11] employing domain imaging techniques. The use of a layer resolved photoelectron emission microscopy supported by the element specific x-ray magnetic circular dichroism (XMCD) provided quantitative information on the domain formation and the canting of the Ni layers within the remanent state. The dependence on the Cu spacer thickness, i.e. the strength of the interlayer coupling, has also been addressed. To study the thermodynamic ground state of such a trilayer and get insight into the competing in- and out-of-plane magnetic anisotropy energies (MAE), it is necessary to apply a static external magnetic field and measure the angular dependence of the free energy. With ferromagnetic resonance (FMR) one obtains full information on the equilibrium angles, anisotropies, and the interlayer exchange coupling. Here we will use well-known theory based on the Landau–Lifshitz equation to provide a detailed interpretation of our investigation on exchange coupled Cu/Ni/Cu/Co/Cu(001) trilayers with mutually perpendicular easy axes. We use the *in situ* ultrahigh vacuum (UHV) FMR technique to benefit from preparing and measuring the trilayer structure step-by-step. Thereby, we firstly get absolute anisotropy values for the bottom layer and, after coupling it to the second magnetic layer, this results in an absolute measure of the interlayer coupling strength of the *same* film [2]. This is not possible in *ex situ* set-ups, since two similarly prepared ultrathin films will hardly ever have the same anisotropies, as can be seen in the following (differences up to 10%).

In section 2 we discuss the theoretical predictions on the polar angular dependence of the resonance field and equilibrium angles for different values of  $J_{\text{inter}}$ . A positive sign denotes FM coupling, whereas a negative sign means antiferromagnetic coupling. In the experiment, this value can be tuned by the spacer thickness  $d_{\text{Cu}}$  and shows in most systems an oscillatory behaviour [4, 6, 12–14].

In section 3 we present FMR measurements corresponding to the theory discussed. The Cu/Ni/Cu<sub>x</sub>/Co/Cu(001) trilayers were prepared in UHV with variable spacer thickness ( $2 \text{ ML} < x < 50 \text{ ML}$ ), implying different coupling values  $J_{\text{inter}}$ , and constant thicknesses of Ni (9 ML), Co (1.8 ML), and Cu cap (5 ML). To simplify the notation, the layer thicknesses will be written as subscripts (e.g. Ni<sub>9</sub>Cu<sub>5</sub>Co<sub>1.8</sub>). All trilayers were grown on a Cu(001) substrate (omitted in the following).

## 2. Theory

### 2.1. FMR in a trilayer with $J_{\text{inter}} = 0$

Figure 1 illustrates the trilayer system with its coordinate system. The microwave field is applied along the film plane, while the external magnetic field  $\mathbf{H}$  is applied perpendicularly to the microwave in the  $yz$ -plane at the polar angle  $\theta_H$  measured with respect to the film normal.  $\theta_1^{\text{eq}}$  and  $\theta_2^{\text{eq}}$  denote the polar equilibrium angles of each magnetization ( $\mathbf{M}_1$ ,  $\mathbf{M}_2$ ). Therefore its azimuthal angle  $\varphi_H$ , measured with respect to the  $[1\ 0\ 0]$  axis, is always constant ( $\varphi_H = 45^\circ$ ).

The angular dependence of the resonance field  $H_{\text{res}}$  of a single magnetic film can be obtained by solving the Smit and Beljers [15] equation

$$\left(\frac{\omega}{\gamma}\right)^2 - \frac{(F_{\theta\theta} - F_{\varphi\varphi} - F_{\theta\varphi}^2)}{M^2 \sin^2 \theta^{\text{eq}}} = 0 \quad (1)$$

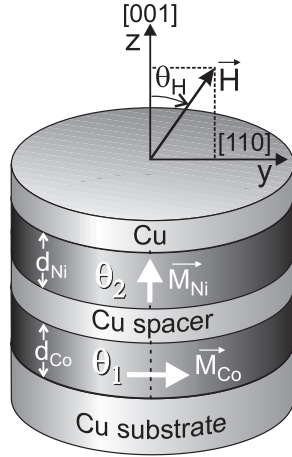


Figure 1. Sketch of the trilayer structure and its coordinate system.

for the free energy density

$$F = [-MH \cos(\theta_H - \theta) + (2\pi M^2 - K_2) \cos^2 \theta - \frac{1}{8} K_{4\parallel} (3 + \cos 4\varphi) \sin^4 \theta] \quad (2)$$

together with the equilibrium condition  $\partial F / \partial \theta = 0$ . In equation (2)  $\theta$  is the polar angle of the magnetization  $M$ ,  $\varphi$  its azimuthal angle,  $F_{\theta\theta}$  is the second partial derivative of  $F$ ,  $K_2$  is the uniaxial anisotropy constant, and  $K_{4\parallel}$  is the fourfold in-plane anisotropy constant. We only use effective anisotropy values  $M_{\text{eff}} = 2K_{2\perp}/M - 4\pi M$ . This implies the assumption of a demagnetizing field of an infinitely thin disc which for the 9 ML Ni film is valid. For the thinner Co film this gives a factor of 0.9 [16] neglected here. Since the angular dependences depend only on  $M_{\text{eff}}$ , the coupling values are not affected by this assumption. We will always assume  $\varphi = 45^\circ$ , i.e. the rotation of  $M$  in the vertical  $(1 \bar{1} 0)$  plane, since the in-plane anisotropy fields are usually much smaller than the resonance field.

In figure 2(a), the two solid curves show the result of the resonance equation for a single Co film with negative  $K_2$ , i.e. in-plane easy axis, and a single Ni film with out-of-plane easy axis. Each line shows a simple  $180^\circ$  symmetry. The visible crossing of the Ni and Co  $H_{\text{res}}(\theta_H)$  curves at  $\theta_H \approx 18^\circ$  is expected, because the magnetic field is applied in the easy direction of Co for  $\theta_H = 90^\circ$  (low resonance field) while the easy direction of Ni is  $\theta_H = 0^\circ$ .

## 2.2. FMR in a coupled trilayer with $J_{\text{inter}} \neq 0$

Now we include the interlayer exchange coupling  $J_{\text{inter}}$ . The free energy is now rebuilt to the form

$$F = \sum_{i=1}^2 d_i [-M_i H \cos(\theta_H - \theta_i) - (2\pi M_i^2 - K_2^i) \sin^2 \theta_i + F_{K_i}] + F_{\text{inter}} \quad (3)$$

with

$$F_{K_i} = -\frac{1}{8} K_{4\parallel}^i (3 + \cos 4\varphi_i) \sin^4 \theta_i \quad (4)$$

and

$$F_{\text{inter}} = -J_{\text{inter}} \cos(\theta_1 - \theta_2) \quad (5)$$

where  $d_i$  is the thickness of the Co ( $i = 1$ ) or Ni ( $i = 2$ ) film. The equilibrium conditions are  $\partial F / \partial \theta_i = 0$  with the minimum determined by checking always for  $F_{\theta_i \theta_i} > 0$  and

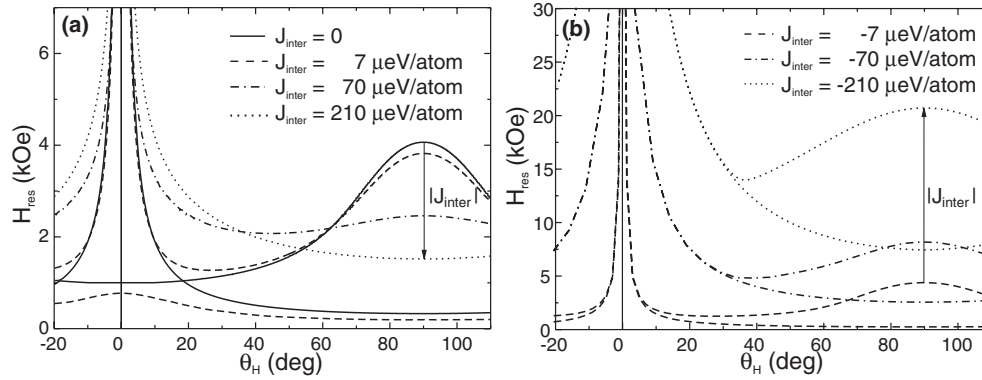


**Figure 2.** Calculated angular dependent resonance field for different values of  $J_{\text{inter}}$  for (a) FM and (b) AFM coupling at 9 GHz. The solid curves in (a) show the results for two uncoupled films. With increasing  $J_{\text{inter}}$  in (a) the acoustical mode shifts down and the optical mode shifts to  $H \rightarrow 0$ , whereas in (b) both modes move to higher fields.

$F_{\theta_1\theta_1}F_{\theta_2\theta_2} - F_{\theta_1\theta_2}^2 > 0$ . The resulting rather long resonance equation has been discussed elsewhere [17].

The influence of FM coupling on the  $H_{\text{res}}(\theta_H)$  curves is demonstrated in figure 2(a) for  $J_{\text{inter}} = 7, 70, \text{ and } 210 \mu\text{eV}/\text{atom}$ . It should be emphasized that now the two  $H_{\text{res}}(\theta_H)$  curves can no longer be treated as independent Co or Ni precessions but rather as two different modes, both involving the Co and Ni magnetizations. Both magnetizations may precess in-phase (out-of-phase) corresponding to the acoustical (optical) mode. In the case of FM coupling, the mode at higher (lower) field is the acoustical (optical) and vice versa in the case of AFM coupling. However, the maximum at  $90^\circ$  is still influenced by the Ni anisotropy and that at  $0^\circ$  by the Co anisotropy. One can see that by including a coupling the two modes are split over the whole range of  $\theta_H$  (no more level crossing) and the splitting increases with the strength of the coupling. Simultaneously, for  $\theta_H$  close to the in-plane configuration, both modes shift to lower resonance fields and, in the limit of a large  $J_{\text{inter}}$ , only the acoustical mode stays visible and shifts to an intermediate position. There the Co and Ni film become rigidly coupled and thus behave like a single averaged film with only one precessing magnetization [18, 19]. It should be noticed that, in this case, the use of the shape anisotropy of the individual layers is still applicable [18]. Figure 2(b) shows the corresponding case for AFM coupling with  $J_{\text{inter}} = -7, -70, \text{ and } -210 \mu\text{eV}/\text{atom}$ . Here both modes move toward higher  $H_{\text{res}}$  values for increasing coupling, and thus stay visible for all values of  $J_{\text{inter}}$  provided that the magnetic field can be made large enough. Moreover, they approach each other with decreasing  $\theta_H$ . However, it should be emphasized that, in the limit of a large AFM coupling, again only one mode will be visible due to the decrease in the intensity of the optical mode with increasing coupling strength [19].

By evaluation of the free energy we also get the equilibrium angles  $\theta_i^{\text{eq}}$  shown in figure 3 for three typical cases:

- (i) Weak FM coupling is presented in figure 3(a). Here, the dashed (solid) curves correspond to the directions of the magnetization in the Co (Ni) film for the two modes visible in figure 2(a). For  $\theta_H = 90^\circ$  one pair of magnetization vectors is aligned collinearly at  $90^\circ$ , forming the acoustical mode.  $\theta_1 = \theta_2 = 90^\circ$  means that both magnetizations lie in the film plane. This is due to the much larger negative perpendicular anisotropy of the Co film

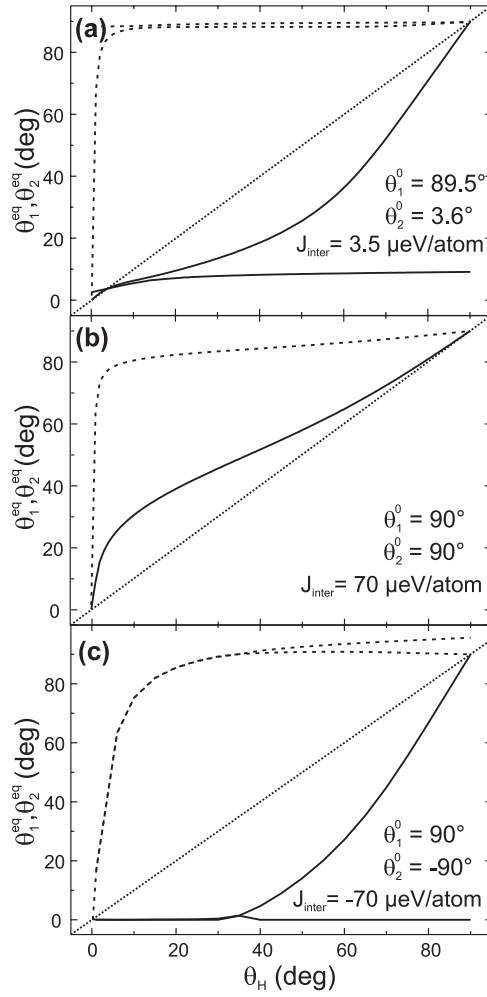


**Figure 3.** Calculations of the equilibrium angles  $\theta_1^{\text{eq}}$  (solid) and  $\theta_2^{\text{eq}}$  (dashed) for different values of  $\theta_1^0$  (a, b) FM and (c) AFM coupling. The dotted line (identity) is a guide to the eye indicating the paramagnetic behaviour for an isotropic film.  $\theta_{1,2}^0$  represent the equilibrium angles at zero field.

which forces the Ni magnetization to be in-plane, parallel to the external field. When  $\theta_H$  is decreased, the direction of one of the Ni angles starts immediately to turn into the out-of-plane direction (faster than the external field), due to its positive perpendicular anisotropy. The Co direction stays in-plane (its easy direction) within a wide angular range until the stronger external field (see figure 2(a)) overcomes the effective Co field and therefore turns it into the easy direction of Ni. The other mode shows almost no angular dependence and thus can be correlated to the optical mode which needs a higher energy (or lower  $H_{\text{res}}$ ) to be excited. This weak FM coupling results in a slightly canted state, since the coupling is not strong enough, to favour a parallel alignment but, on the other hand, it is already large enough to tilt the magnetization direction against the anisotropies. The equilibrium angles  $\theta_i^0$  at zero field ( $H = 0$ ) are also given in figure 3 thus denoting the natural state of the system without an external magnetic field. Here, for weak FM coupling the magnetization vectors stay almost perpendicular ( $85.9^\circ$ ) to each other.

- (ii) With intermediate FM coupling (see figure 3(b)) they line up in parallel without an external magnetic field. As already seen in figure 2(a) the optical mode vanishes. Now the coupling between the films is strong enough to retard the rotation of the Ni direction while decreasing  $\theta_H$ . On the other hand, the Co direction turns a little faster out-of-plane compared to a weak coupling. In the limit of a very strong coupling the dashed and the solid curve would approach each other and fall together showing the behaviour of a single film only. In zero fields both magnetizations are aligned parallel in-plane as expected.
- (iii) In the case of intermediate AFM coupling, shown in figure 3(c), the Ni direction turns much faster out-of-plane than the external field, because  $J_{\text{inter}}$  prefers an antiparallel alignment and thus the large effective field of the Co film pushes the Ni magnetization faster to its intrinsic out-of-plane direction. Nevertheless, an antiparallel alignment of both magnetizations is not visible, except for  $H = 0$ . Secondly, below  $\theta_H \approx 36^\circ$ , both modes approach each other resulting in only one visible resonance line as shown in figure 2(b). This angle increases asymptotically with increasing AFM coupling strength. However, the absolute value of the asymptote (in our system  $\approx 36^\circ$ ) is subject to the interplay of the anisotropies and the interlayer exchange coupling.

### 3. Experimental results and discussion

The FMR measurements were performed at 9 GHz. Technical details are described elsewhere [12, 20]. Preparation and FMR were done at room temperature in an UHV system [2] with a base pressure of  $5 \times 10^{-11}$  mbar. In a first step 1.8 ML Co were epitaxially grown on a Cu(001) single crystal and subsequently capped with the Cu spacer. This system was then annealed for 10 min at  $T = 440$  K to smooth the spacer. The film growth was monitored by MEED (medium energy electron diffraction) oscillations ( $\approx 1$  ML  $\text{min}^{-1}$ ) and AES (Auger electron spectroscopy). For this system the polar angular dependence of the single resonance mode was measured to determine the anisotropy values of the Co film which show a clear in-plane easy axis of magnetization. Due to the limiting magnetic field, a small angular range around the perpendicular orientation could not be measured. To complete the trilayer system with easy axes perpendicular to each other, 9 ML Ni with a Cu cap of 5 ML were evaporated in a second step. As is known, Ni undergoes a transition from the in-plane to the perpendicular magnetization direction above 8 ML when capped with Cu [21]. The Co film stays in-plane over the whole thickness range. Additionally, this Co thickness allows room temperature studies because the  $T_C$  of 2 ML Co is about 340 K. Thinner Co films exhibit a lower anisotropy (better for magnetic measurements), which already for 2 ML is  $M_{\text{eff}} = -42$  kG, but below 1.8 ML of Co the  $T_C$  jumps down to 200 K [22]. For comparison, the effective magnetization of a 9 ML Ni film is equal to  $M_{\text{eff}} = -1.9$  kG.

Now, in this trilayer system, both coupled magnetizations precess either in-phase or out-of-phase giving the two resonance modes as described in section 2. In figure 4 two examples of trilayers with (a) weak ( $d_{\text{Cu}} = 6.5$  ML,  $J_{\text{inter}} = 5.95$   $\mu\text{eV}/\text{atom}$ ) and (b) very strong ( $d_{\text{Cu}} = 2.5$  ML,  $J_{\text{inter}} = 1120$   $\mu\text{eV}/\text{atom}$ ) FM coupling are shown. As expected from the theory discussed above, both modes in the left panel are still visible and show no crossing. In the right panel only the acoustical mode is left. The inset shows the FMR signal at  $\theta_H = 90^\circ$  before and after preparation of the second magnetic layer. It should be noticed that the single film resonance depicted by the dotted curve disappears at  $H = 0$  and does not correspond to the resonance peak visible after deposition of the Ni film (solid curve). The related anisotropy values are given in table 1. An explanation for the large coupling value at 2.5 ML spacer thickness might be that both magnetic layers are not entirely confined by the Cu spacer but are partly in contact due to roughness or interdiffusion. Although this is not quite the same

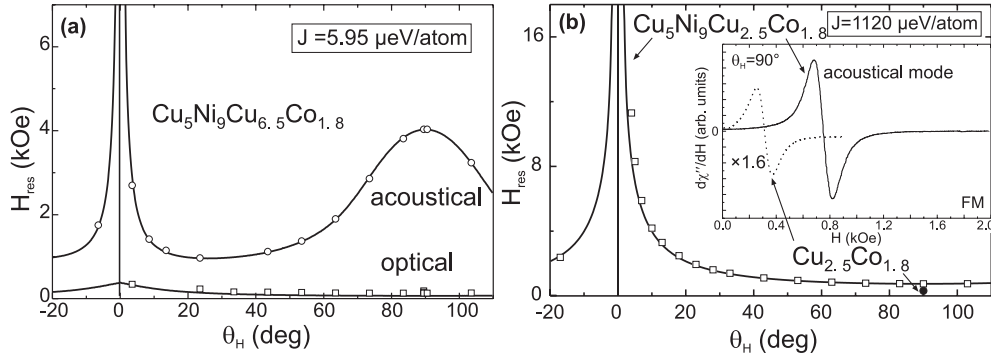


**Figure 4.** (a) Angular dependence of the resonance field with respect to the polar angle  $\theta_H$  for weak FM coupling ( $J_{\text{inter}} = 5.95 \mu\text{eV}/\text{atom}$ ) in  $\text{Cu}_5\text{Ni}_9\text{Cu}_{6.5}\text{Co}_{1.8}$ . Circles correspond to the acoustical mode, squares to the optical mode. The zero-field equilibrium angles are  $\theta_1^0 = 89.4^\circ$  and  $\theta_2^0 = 5.6^\circ$ . (b) Experimental data for strong FM coupling ( $J_{\text{inter}} = 1120 \mu\text{eV}/\text{atom}$ ) in  $\text{Cu}_5\text{Ni}_9\text{Cu}_{2.5}\text{Co}_{1.8}$ . The optical mode has shifted to  $H \rightarrow 0$ . The zero-field equilibrium angles are both  $\theta_{1,2}^0 = 90^\circ$ . The inset shows the corresponding FMR spectra for  $\theta_H = 90^\circ$ . The dotted curve denotes the signal for the Co film only, whereas the solid curve is the acoustical mode of the coupled system.

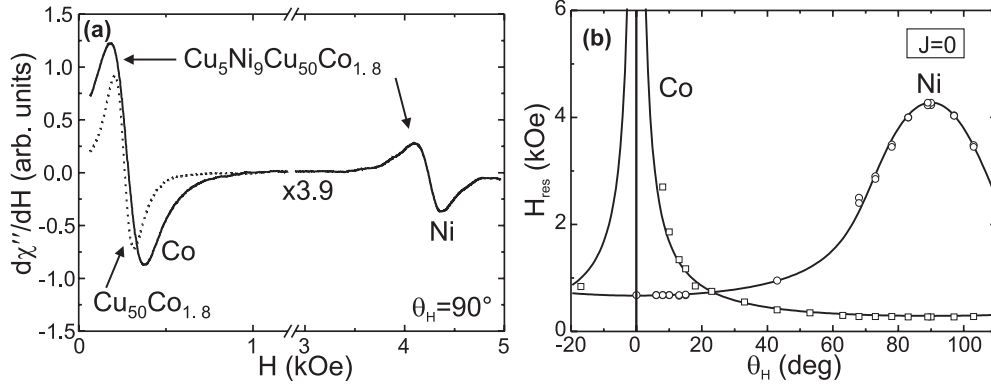


**Figure 5.** (a) FMR spectra at  $\theta_H = 90^\circ$  for the Co film (dotted) and for the (in this case) uncoupled trilayer system (solid). (b) The corresponding angular dependence of the resonance field for the  $\text{Cu}_5\text{Ni}_9\text{Cu}_{50}\text{Co}_{1.8}$  trilayer. The circles belong to the Ni layer, whereas the squares show the Co data. The solid curves are fits.

**Table 1.** Measured anisotropy values and coupling strength for the different films.

System	$M_{\text{eff}}^{\text{Co}}$ (kG)	$K_{4\parallel}^{\text{Co}}/M$ (kG)	$M_{\text{eff}}^{\text{Ni}}$ (kG)	$K_{4\parallel}^{\text{Ni}}/M$ (kG)	$J_{\text{inter}}$ ( $\mu\text{eV}/\text{atom}$ )
$\text{Cu}_5\text{Ni}_9\text{Cu}_{50}\text{Co}_{1.8}$	-26.3	-0.019	2.26	-0.062	0
$\text{Cu}_5\text{Ni}_9\text{Cu}_{6.5}\text{Co}_{1.8}$	-37.6	-0.025	2.24	-0.103	5.95
$\text{Cu}_5\text{Ni}_9\text{Cu}_{2.5}\text{Co}_{1.8}$	-38.9	—	1.98	—	1120
$\text{Cu}_5\text{Ni}_9\text{Cu}_{4.5}\text{Co}_{1.6}$	-26.2	0.041	1.53	-0.103	-1.05

system as presented in [17], one might compare the coupling strength qualitatively, since the oscillation period is mainly determined by the spacer material. Therefore, a large FM coupling is reasonable, too.



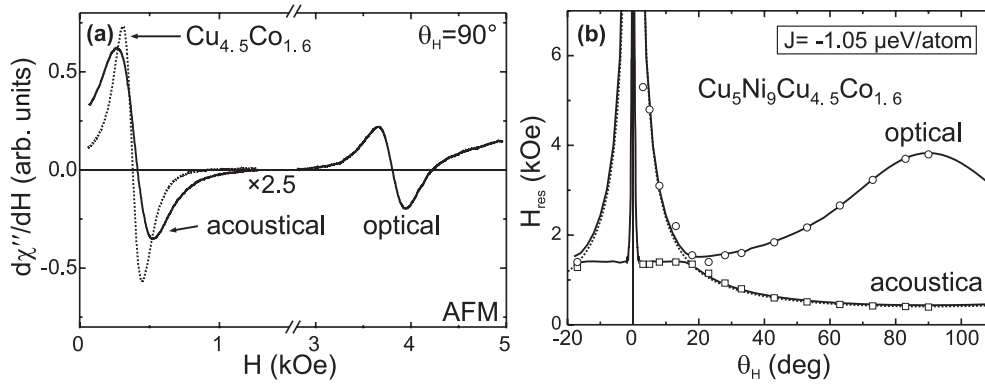


**Figure 6.** (a) FMR spectra at  $\theta_H = 90^\circ$  for  $\text{Cu}_5\text{Ni}_9\text{Cu}_{4.5}\text{Co}_{1.6}$  and (b) the corresponding angular dependence of the resonance field with respect to the polar angle  $\theta_H$  for weak antiferromagnetic coupling of  $J_{\text{inter}} = -1.05 \mu\text{eV}/\text{atom}$ . The zero-field equilibrium angles are  $\theta_1^0 = 90.3^\circ$  and  $\theta_2^0 = -1.3^\circ$ . The dotted curves represents the lower film only.

For comparison we show in figure 5 the FMR signal with the external field  $H$  applied in-plane for the  $\text{Cu}_5\text{Ni}_9\text{Cu}_{50}\text{Co}_{1.8}$  system yielding the uncoupled case due to its thick Cu spacer. In figure 5(a) the dotted curve shows the uniform mode of the Co film as measured in the first step. The solid curve shows the signal of the trilayer system. Since there is almost no shift in the resonance of the Co signal, the Co and Ni magnetizations are uncoupled and can be described independently. Figure 5(b) shows the corresponding polar angular dependence. Co (open squares) shows the expected in-plane easy axis (weak resonance field at  $\theta_H = 90^\circ$ ), whereas Ni (open circles) is magnetized out-of-plane (weak resonance field at  $0^\circ$ ). The solid curves are the theoretical fits described previously (see also the solid curves in figure 2(a)).

Figure 6 shows the FMR signal and the angular dependence of a trilayer with 4.5 ML spacer thickness. Here, both the acoustical and the optical mode are visible over the full angular range. In the left panel one can see that the resonance has shifted upon preparation of the Ni layer to a slightly higher field, revealing a weak antiferromagnetic coupling. The fit of the angular dependence (right panel) gives  $J_{\text{inter}} = -1.05 \mu\text{eV}/\text{atom}$  and the anisotropy values shown in table 1. Since both films are very weakly coupled (a factor of 7 smaller than the calculated example), an approach of optical and acoustical mode, which might be expected for AFM coupling from figure 2(b), is not visible. On the other hand, a large increase in the resonance field of the acoustical mode at perpendicular orientation can be noticed.

From table 1 one can see a significant variation in the values of the  $M_{\text{eff}}$ , mainly in the case of Co. This is expected, because such a thin Co film is certainly sensitive to a small change of its thickness, the quality of the interface, etc. Another observation, which can be seen from table 1, is that the in-plane  $K_{4\parallel}$  term changes its sign when the Co film has a thickness of 1.6 ML. For 1.8 ML of Co the sign is negative (row 2) or the  $K_{4\parallel}$  is negligible (row 3). The accuracy of the Co thickness determination is about 0.1 ML, which means that, at about  $1.7 \pm 0.1$  ML of Co, there might be a reorientation of the in-plane easy axis from  $[1\ 0\ 0]$  to  $[1\ 1\ 0]$ , which is reflected in the change of sign of  $K_{4\parallel}^{\text{Co}}$ . To our knowledge the in-plane properties, in particular the anisotropies of the Co films below 1.8 ML thickness, have not been investigated in detail so far. Therefore, the unambiguous identification of the reorientation is left for future studies. Additionally, in the case of row 3, the fitting procedure is not very sensitive to the in-plane anisotropy parameters of Co and Ni because the extremely large coupling dominates any small contributions. One should note that both observations can

only be made because of our fully *in situ* and step-by-step characterization, by which it is possible to get the real values of the parameters included in the table. The widely used method based on a one-step *in situ* preparation of the system and further *ex situ* studies of  $J_{\text{inter}}$  makes use of reference single films for the anisotropy values. However, this would not provide such reasonable results.

#### 4. Conclusion

High quality  $\text{CuNiCu}_x\text{Co}/\text{Cu}(001)$  films exhibiting in-plane Co and perpendicular Ni easy axes have been prepared. We have shown that, for these trilayers, a comprehensive theoretical description can be given. The *in situ* measured angular dependence of the in-phase and out-of-phase resonance modes was successfully analysed providing the equilibrium orientations of the magnetizations within these modes. The individual orientation of the Ni as well as Co magnetization depends on two parameters: the strength and orientation of the external field plus the exchange and anisotropy fields. It has been found that the strong intrinsic anisotropies preferring a mutual  $90^\circ$  orientation of the magnetization prevent the appearance of a clear antiparallel alignment usually expected for large values of coupling. The *in situ* FMR technique confirmed its advantage in determining absolute interlayer coupling values.

#### Acknowledgments

We thank A N Anisimov for providing the analysis software. This work was supported by the DFG (Sfb290, TP A2) and BMBF (KS1 KEB4).

#### References

- [1] Bürgler D E, Buchmeier M, Cramm S, Eisebitt S, Gareev R R, Grünberg P, Jia C L, Pohlmann L L, Schreiber R, Siegel M, Qin Y L and Zimina A 2003 *J. Phys.: Condens. Matter* **15** S443
- [2] Lindner J and Baberschke K 2003 *J. Phys.: Condens. Matter* **15** R193
- [3] Rezende S M, Chesman C, Lucena M A, de Moura M C, Azevedo A, de Aguiar F M and Parkin S S P 1999 *J. Appl. Phys.* **85** 5892
- [4] Heinrich B, Cochran J F, Kowalewski M, Kirschner J, Celinski Z, Arrott A S and Myrtle K 1991 *Phys. Rev. B* **44** 9348
- [5] Strijkers G J, Kohlhepp J T, Swagten H J M and de Jonge W J M 2000 *Phys. Rev. Lett.* **84** 1812
- [6] Grünberg P, Schreiber R, Pang Y, Brodsky M B and Sowers H 1986 *Phys. Rev. Lett.* **57** 2442
- [7] Zhang Z, Zhou L, Wigen P E and Ounadjela K 1994 *Phys. Rev. Lett.* **73** 336
- [8] Zhang Z, Zhou L, Wigen P E and Ounadjela K 1994 *Phys. Rev. B* **50** 6094
- [9] Kuch W, Gao X and Kirschner J 2002 *Phys. Rev. B* **65** 064406
- [10] Kuch W, Gilles J, Gao X and Kirschner J 2002 *J. Magn. Magn. Mater.* **242–245** 1246
- [11] Kuch W, Chelaru L I, Fukumoto K, Porrati F, Offi F, Kotsugi M and Kirschner J 2003 *Phys. Rev. B* **67** 214403
- [12] Lindner J, Kollonitsch Z, Kosubek E, Farle M and Baberschke K 2001 *Phys. Rev. B* **63** 094413
- [13] Bruno P 1995 *Phys. Rev. B* **52** 411
- [14] Baibich M N, Broto J M, Fert A, Nguyen Van Dau F, Petroff F, Eitenne P, Creuzet G, Friederich A and Chazelas J 1988 *Phys. Rev. Lett.* **61** 2472
- [15] Smit J and Beljers H G 1955 *Philips Res. Rep.* **10** 113
- [16] Heinrich B 1994 *Ultrathin Magnetic Structures* vol 2, ed J A C Bland and B Heinrich (Heidelberg: Springer) pp 200–2
- [17] Lindner J and Baberschke K 2003 *J. Phys.: Condens. Matter* **15** S465
- [18] Layadi A and Artman J O 1990 *J. Magn. Magn. Mater.* **92** 143
- [19] Layadi A and Artman J O 1997 *J. Magn. Magn. Mater.* **176** 175
- [20] Farle M 1998 *Rep. Prog. Phys.* **61** 755
- [21] Baberschke K and Farle M 1997 *J. Appl. Phys.* **81** 5038
- [22] Pouloupoulos P, Jensen P J, Ney A, Lindner J and Baberschke K 2002 *Phys. Rev. B* **65** 064431